

1 **Fitting Bayesian state-space biomass dynamics models to standardized CPUE for carpenter**
2 **and silver kob stocks**

3

4 H Winker¹, AJ Booth², SE Kerwath^{3,1} and CG Attwood¹

5 ¹*Zoology Department, University of Cape Town, Private Bag Rondebosch 7700, South Africa.*

6 ²*Department of Ichthyology and Fisheries Science, Rhodes University, PO Box 94,*
7 *Grahamstown 6140, South Africa*

8 ³*Marine and Coastal Management, Private Bag X2, Roggebaai 8012, South Africa*

9

10 **Introduction**

11 The South African boat-based, commercial linefish sector refers to a multi-species, multi-area
12 cluster of low to medium technology boat-based inshore fisheries in which more than 200 fish
13 species are caught manually by hand-lines or rods and reels. Within this cluster one can identify
14 individual fisheries on the basis of fishing strategy, area and target species, but other fisheries
15 such as the demersal trawl fishery also impact on the resource given the considerable overlap in
16 terms of catch compositions (Attwood et al., 2011). The species that account for the largest
17 landings by the linefishery can be roughly grouped into pelagic shoaling species such as
18 yellowtail (*Seriola lalandi*) and snoek (*Thyrsites atun*), demersal species such as silver kob
19 (*Argyrosomus inodorous*) and geelbek (*Atractoscion aequidens*) and reef-associated seabreams
20 including carpenter (*Argyrozona argyrozona*), slinger (*Chrysoblephus puniceus*) and hottentot
21 (*Pachymetopon blochii*).

22

23 Monitoring of the linefishery started at the turn of the 20th century with JDF Gilchrist, the
24 Government Marine biologist of the Cape of Good Hope, and the first concerns about
25 overfishing of some linefish species were voiced already in the 1940s (Griffiths 2000).
26 Mandatory catch and effort returns from the boat-based commercial linefishery have been
27 captured since 1985 and stored in the National Marine Linefish System (NMLS), a database
28 hosted by the South African Department of Agriculture, Forestry and Fisheries (DAFF). In 1985,
29 the linefish sector was also formally recognized for the first time and national legislation was
30 introduced to limit effort and fishing mortality. Despite these first regulations, spawner-biomass
31 per-recruit analyses and comparisons with historical catch data in the 1990s indicated alarming
32 states for many linefish stocks (Buxton, 1992; Punt, 1993; Punt et al., 1996; Griffiths, 1997;
33 Griffiths, 2000), which subsequently lead to the declaration of a state of emergency in this
34 fishery in 2000, accompanied by a significant reduction in commercial boat effort (nominally ~
35 70%). The forced reduction of effort was reflected in the allocation of medium-term and long-
36 term commercial fishing rights and in the formulation of the linefish management protocol
37 (Griffiths 1997a), which intended to guide the management of stocks according to biological
38 reference points based on spawner biomass per-recruit models.

39

40 Several linefish species have been assessed once by spawner-biomass per-recruit analysis. This
41 first wave of assessments was to estimate the relative depletion levels of the stocks, many of
42 which had been exploited for a century by the fishery (Griffiths, 2000). However, there has been
43 no attempt to assess and quantify the impact of the ensuing reduction of commercial effort in
44 2000, which was designed to rebuild stocks. To date, more than a decade later, there is therefore
45 a pressing need for a new round of linefish assessments. Per-recruit analysis might not be

46 appropriate to quantify a potential recovery of stocks as it relies on the steady-state assumptions
47 of constant fishing mortality and constant recruitment, which will almost certainly be violated in
48 the case of stock rebuilding (Butterworth et al., 1989). Despite catch and effort data being
49 captured since 1985, linefish stock assessment in South Africa has previously been hampered by
50 the inability to standardize the catch-per-unit-effort (CPUE) time series for the effect of
51 multispecies targeting. Recent developments of standardization approaches for multispecies
52 CPUE now permit constructing more reliable time series of abundance indices with potentially
53 useful information for stock assessments (Winker et al., 2012; Winker et al., accepted).

54

55 The objective of this study was to assess stock status of carpenter and silver kob twelve years
56 after the emergency in the linefishery. To achieve this, we developed Bayesian state-space
57 biomass dynamic (surplus production) models, which were fitted to time series of landings data
58 and standardized abundance indices. We chose biomass dynamics models because there was
59 insufficient age-disaggregated data available to employ more complex age-structured models.
60 The fairly low data requirements of biomass dynamics models make them an attractive option in
61 situations where reliable information about the size- and age-structure of the stock is difficult to
62 obtain (Hilborn and Walters, 1992). State-space models are regarded as a powerful tool for
63 modelling time-varying abundance indices because they simultaneously account for both process
64 error and observation error (Meyer and Millar, 1999; de Valpine, 2002; Buckland et al., 2004).
65 The process error can account for model structure uncertainty as well as natural variability of
66 stock biomass due to stochasticity in recruitment, natural mortality, growth and maturation,
67 while the observation error determines the uncertainty in the observed abundance index due to
68 reporting error and unaccounted variations in catchability (Meyer and Millar, 1999; Buckland et

69 al., 2004; Ono et al., 2012). A Bayesian framework was chosen to reduce uncertainties about
70 estimates of stock size, fishing mortality and fisheries reference points through the use of
71 informed priors (Punt and Hilborn, 1997; Hilborn and Liermann, 1998; McAllister et al., 2001),
72 which incorporate published literature on historical stock levels and population demographics.
73 The main output of the assessment models are biplots that simultaneously portray the trajectory
74 of the exploited stock against target population size and target harvest rate at Maximum
75 Sustainable Yield (MSY) for the period from 1987 to 2012.

76

77 **Materials and methods**

78 *Data*

79 Catch and effort data for the boat-based South African handline fishery were extracted from the
80 National Marine Linefish System (NMLS) and total landing reported by the inshore trawl fleet
81 were obtained from the Department of Agriculture, Forestry and Fishery (DAFF). The time
82 series considered for the analysis was 1987 – 2011. The catches from both fisheries were
83 aggregated by region assuming that the populations of both species can be split into a southern
84 stock and a south-eastern stock (Fig 1). The magnitude of the carpenter and silver kob catches
85 that are discarded by the inshore trawl fleet has been estimated based on based on on-board
86 observer data collected during the period from 2003 to 2006 (Attwood et al., 2011). To account
87 for discard mortality in the assessment models, the reported trawl landings for carpenter and
88 silver kob were multiplied by the estimated pre-discard to post-discard catch ratios of 2.61 and
89 1.49, respectively (Attwood et al., 2011).

90

91 Standardized CPUE time series (1987-2011) were based on commercial hand-line catch and
 92 effort data. The raw data comprised mandatory daily catch returns (kg) per species per boat day
 93 as estimated by the skipper, vessel number, crew number, hours on sea, the date and catch
 94 location. The reported catch location, initially provided as a shore position and a distance
 95 offshore, is referenced to the midpoints of 5×5 minute latitude and longitude grid-cells. The
 96 CPUE data were standardized by following the standardization approach described for carpenter
 97 and silver kob in Winker et al. (in press). This approach involves the application of a
 98 Generalized Additive Model framework that was designed to adjust for the effect of different
 99 fishing tactics by making use of the information contained in the catch composition. Additional
 100 predictor variables included in the model are year, month, latitude (lat) and longitude (long),
 101 crew size (crew) and mean hours spent at sea per record (hours). For this analysis, the CPUE
 102 records for the southern stock were subset into two regions, south-west and south-central (SC), to
 103 reflect the geographical division of the fishery and to account for geographical differences in
 104 species composition and targeting (Fig.1).

105

106 *State-space biomass dynamics model*

107 Three principle classes of non-equilibrium estimation frameworks have been widely used for
 108 biomass dynamics models: (1) observation error model, (2) process error models and (3) total
 109 error models (Polachek et al., 1993; Punt, 2003). A generic formulation for biomass dynamics
 110 models can be written as:

$$111 \quad B_{t+1} = (B_t + g(B_t | \theta) - C_t) \exp(\eta_t)$$

$$112 \quad I_t = qB_t \exp(\epsilon_{t,j})$$

113

114 where B_t is the biomass at the start of year t , $g(B_t | \boldsymbol{\theta})$ denotes the surplus production as
 115 function of B_t and a given vector of parameters $\boldsymbol{\theta}$, C_t is the catch in year t (assumed be known),
 116 I_t is the relative index of abundance in year t , q the catchability coefficient scaling the modelled
 117 biomass to the abundance index I_t , and η_t is the process error in year t and $\varepsilon_{t,i}$ is the observation
 118 error for year t in abundance index, with $\eta_t \sim N(0, \sigma^2)$ and $\varepsilon_{t,i} \sim N(0, \tau_i^2)$, respectively.

119

120 Each of the three estimation frameworks represents a special case of the generalized model
 121 defined by equations (1) and (2), with $\tau^2 = 0$ in the case of process error models, $\sigma^2 = 0$ in the
 122 case of observation error models, and a predefined relationship between σ^2 and τ^2 (i.e. $\sigma^2 / \tau^2 =$
 123 C) in the case of total error models (Punt, 2003). By contrast, state-space models do not require
 124 assumptions about a fixed relationship between σ^2 and τ^2 , as they are based on likelihood
 125 calculations that can integrate over unknown process errors (Meyer and Millar, 1999; Millar and
 126 Meyer, 2000; de Valpine, 2002; Punt, 2003). Most recent advances in random effects modelling
 127 now allow for treating the process errors as a vector of unobserved random effects $\boldsymbol{\eta} = \{\eta_1 \dots \eta_n\}$
 128 that can be integrated out when estimating the process error variance σ^2 (Fournier et al., 2012;
 129 Ono et al., 2012; Pedersen et al., 2012; Thorson et al., 2012). This procedure is implemented in
 130 the open source software ADMB-RE (Fournier et al., 2012; <http://admb-project.org>), which
 131 provides a computationally efficient way to implement state-space models (Pedersen et al.,
 132 2012).

133

134 Here, we develop a numerically integrated Bayesian state-space model according to Meyer and
 135 Millar (1999), by using the mixed-effect modelling framework in ADMB-RE (Fournier et al.,

136 2012; Pedersen et al., 2012). The production function is assumed to follow the Schaefer (1954)

137 or logistic form:

$$138 \quad g(B_t) = rB_t \left(1 - \frac{B_t}{K} \right),$$

139 where r is the intrinsic rate of population increase and K is the biomass at the carrying capacity.

140 As the exploitation of many linefish species commenced already in the mid-1800s, it would be

141 unrealistic to assume that the biomass at the start of the time series in 1987 approximates the

142 pristine biomass prior to exploitation K . The initial biomass in the first year of the time series

143 was therefore scaled by introducing the model parameter φ , which is defined by the ratio of the

144 biomass in the first year of the CPUE time series to K , such that:

145

$$146 \quad B_1 = \varphi K \exp(\eta_1)$$

$$147 \quad B_t = \left(B_{t-1} + rB_{t-1} \left(1 - \frac{B_{t-1}}{K} \right) - C_{t-1} \right) \exp(\eta_t) \quad t = 2, 3, \dots, n$$

148 As suggested by Meyer and Millar (1999), we re-parameterized the biomass dynamics model by

149 expressing B_t as proportion of K ($P_t = B_t / K$) to improve the efficiency of the estimation

150 algorithm. The stochastic form of the process equation is then:

$$151 \quad P_1 = \varphi \exp(\eta_1)$$

$$152 \quad P_t = \left(P_{t-1} + rP_{t-1} (1 - P_{t-1}) - C_{t-1} / K \right) \exp(\eta_t) \quad t = 2, 3, \dots, n$$

153 and the observation equation is given by:

$$154 \quad I_t = qKP_t \exp(\tau_t) \quad t = 1, 2, \dots, n.$$

155

156

157 *Management quantities*

158 A number of management related quantities were derived to assess the status of the carpenter and
 159 silver kob stocks. These were (1) Maximum Sustainable Yield (MSY), (2) the harvest rate at
 160 MSY (H_{MSY}), (3) the biomass at MSY (B_{MSY}), (4) the depletion as a ratio as biomass in 2012 to
 161 K (B_{2012}/K), (5) the relative change in biomass since the forced effort reduction in 2000
 162 (B_{2012}/B_{2000}) and (6) the ratio of harvest rate in 2012 to the harvest rate that produces MSY at
 163 B_{MSY} (H_{2012}/H_{MSY}), where $MSY = rK/4$, $B_{msy} = K/2$ and $H_{MSY} = r/2$. Stock status trajectories over
 164 the period of the time series (1987 – 2011) are presented in the form of biplot graphs that plot the
 165 ratio B_t/B_{MSY} on the y -axis against the ratio H_t/H_{MSY} on the x -axis, where H_t is the predicted
 166 harvest rate in year t that is calculated as $H_t = C_t / B_t$.

167

168 *Bayesian state-space estimation framework*

169 A fully Bayesian biomass dynamics model projected over n years requires a joint probability
 170 distribution over all unobservable hyper-parameters $\theta = \{K, r, q, \varphi, \sigma^2, \tau^2\}$ and the n process
 171 errors relating to the unobserved random effects vector $\eta = \{\eta_1 \dots \eta_t\}$ (Pedersen et al., 2012),
 172 together with all observable data in the form of the relative abundance indices $\mathbf{I} = \{I_1 \dots I_n\}$
 173 (Meyer and Millar, 1999). Accordingly, the joint posterior distribution of the Bayesian state-
 174 space biomass dynamics model can be conceptually divided into three components: (1) a joint
 175 prior distribution, (2) a distribution for the process equation and (3) a distribution for the
 176 observation equation. The joint prior distribution on the vector of parameters θ is given by:

$$177 \quad p(\theta) = p(K)p(r)p(q)p(\varphi)p(\sigma^2)p(\tau^2)$$

178 Assuming multiplicative log-normal errors, the probability distribution for the process equation
 179 is of the form:

$$180 \quad p(P_1 | \varphi, \sigma^2) \prod_{t=2}^n p(P_t | P_{t-1}, K, r, \varphi, \sigma^2) = \prod_{t=1}^n \left\{ \frac{1}{\sqrt{2\pi\sigma^2}} \exp\left(-\frac{\eta_t^2}{2\sigma^2}\right) \right\},$$

181 and the probability distribution for observation equation, given the unobserved random effects
 182 for year t , η_t , is:

$$183 \quad \prod_{t=1}^n p(I_t | q, K, \tau^2, \eta_t) = \prod_{t=1}^n \left\{ \frac{1}{\sqrt{2\pi(\xi_{t,i}^2 + \tau_i^2)}} \exp\left(-\frac{(\ln(I_t) - \ln(qP_tK))^2}{2(\xi_{t,i}^2 + \tau_i^2)}\right) \right\},$$

184 where $\xi_{t,i}^2$ is observed variance for year t and abundance index I_t , which was calculated from the
 185 standard errors of year effects that were predicted from the CPUE standardization model. In this
 186 approach, the estimated parameter τ^2 corresponds to the additional temporally-invariant variance
 187 in the relative abundance index (Butterworth et al., 1993). According to Bayes' theorem, it
 188 follows that joint posterior distribution over all unobservable parameters, given the data and
 189 unknown random effects, can be formulated as:

$$190 \quad p(\theta | \mathbf{I}, \boldsymbol{\eta}) = p(K)p(r)p(q)p(\varphi)p(\sigma^2)p(\tau_i^2) \\
 \times p(P_1 | \varphi, \sigma^2) \prod_{t=1}^n p(P_t | P_{t-1}, K, r, \varphi, \sigma^2) \times \prod_{t=1}^n p(I_t | q, K, \tau_i^2, \eta_t)$$

191
 192 *Formulation of prior distributions*

193 The formulation of informative prior distributions permits the integration of existent information
 194 from literature into the Bayesian estimation framework. In this way, one can, for example, ensure
 195 that all possible parameter solutions given the data will be within plausible biological limits of
 196 the stock under assessment (McAllister et al., 2001). However, care must be taken not to

197 overstate the precision of priors for uncertain model parameters (Punt and Hilborn, 1997;
 198 McAllister et al., 2001). This typically pertains to parameters of absolute biomass (e.g. K),
 199 catchability or variance estimates, for which it may not be feasible to objectively specify
 200 informative prior distributions given the available information (Punt and Hilborn, 1997;
 201 McAllister et al., 2001; Ono et al., 2012).

202

203 In this study, we assumed non-informative prior distributions for all model parameters except the
 204 intrinsic rate of population increase r and the ratio B_{1987} to K , φ (Table 2). The prior
 205 distributions for σ^2 , τ^2 and K were chosen to be represented by a reasonably uninformative
 206 inverse-gamma distribution:

$$207 \quad p(x) = \frac{\lambda^k x^{-(k+1)}}{\Gamma(k)} \exp\left(-\frac{\lambda}{x}\right),$$

208 with the scaling parameters λ and k set to 0.001 (Chaloupka and Balazs, 2007; Zhou et al.,
 209 2009; Brodziak and Ishimura, 2012). The choice of this distribution implies that the parameters
 210 are approximately uniform on $\ln(x)$ (Jeffrey's prior) and has, for example, the property that lower
 211 weight is assigned to very higher values of K which assists to prevent implausibly large posterior
 212 values of K (McAllister and Kirkwood, 1998). The catchability parameters q are considered to
 213 be uniformly distributed (Booth and Quinn II, 2006). As is common practice, a lognormal was
 214 chosen to determine informative prior distributions $p(\varphi)$ and $p(r)$ (Meyer and Millar, 1999;
 215 McAllister et al., 2001; Brodziak and Ishimura, 2012), such that:

$$216 \quad p(x) = \frac{1}{\sqrt{2\pi x \sigma_{\ln}}} \exp\left(-\frac{(\ln x - \ln \mu)^2}{2\sigma_{\ln}^2}\right),$$

217 where μ denotes prior mean of φ or r and σ_{\ln} is the lognormal standard deviation associated
 218 with $\ln(\mu)$.

219

220 For the base-case scenarios (Model 1), the mean priors for φ were set to $\mu_{\varphi} = 0.15$ and $\mu_{\varphi} = 0.10$
 221 for carpenter and silver kob stocks, respectively. These values are based on the analysis of
 222 historical catch and effort records (1897-1906 and 1927-31) in comparison to catch rates for the
 223 period 1986-1998 and are generally in agreement with estimated spawner-biomass per-recruit
 224 depletion levels (SPR / SPR_0) for both species prior to 2000 (Griffiths, 1997; Brouwer and
 225 Griffiths, 2006). To account for the uncertainty around these estimates, we chose a fairly low
 226 precision associated with μ_{φ} by setting σ_{\ln} to achieve a coefficients of variation (CV) of 40%,
 227 so that $\sigma_{\ln}^2 = \ln(CV^2 + 1)$.

228

229 In order to specify a prior distribution for r , we adapted the Leslie matrix method by McAllister
 230 et al. (2001). Based on this approach, demographic information can be used to construct an age-
 231 structured Leslie matrix \mathbf{A} of the form (Caswell, 2001):

$$232 \quad \mathbf{A} = \begin{pmatrix} \phi_1 & \phi_2 & \phi_3 & \cdots & \phi_{t_{\max}} \\ S_1 & 0 & 0 & 0 & 0 \\ 0 & S_2 & 0 & 0 & 0 \\ 0 & 0 & \ddots & 0 & 0 \\ 0 & 0 & 0 & 0 & S_{t_{\max}-1} \end{pmatrix} \quad (14),$$

233 where ϕ_t is the average number of recruits expected to be produced by an adult female at age t
 234 and S_t is the fraction of survivors at age t . Using matrix algebra, the value of r can be
 235 approximated from the relationship $\lambda = \exp(r)$, where λ is the dominant eigenvalue of the

236 transition matrix (Quinn and Deriso, 1999; Caswell, 2001). Here, we used the basic matrix
 237 analysis tool provided in the Excel add-in ‘Poptools’ (www.poptools.org) to derive λ from the
 238 Leslie matrix, as described in detail by Mollet and Cailliet (2002). The life history parameters
 239 used to construct the prior distributions for r were sourced from previous studies on carpenter
 240 (Brouwer and Griffiths, 2006) and silver kob (Griffiths, 1997) and are summarized in Table 2.

241
 242 Age-dependent survival was estimated as $S_t = \exp(-M)$, where M is the instantaneous rate of
 243 natural mortality. The average number of recruits expected to be produced by an adult female at
 244 age t is expressed as:

$$245 \quad \phi_t = \alpha W_t \psi_t \quad (15),$$

246 where α denotes the slope of the origin of the spawner-recruitment relationship (i.e. the ratio of
 247 recruits to spawner biomass at very low abundance) (Hilborn and Walters, 1992; Myers et al.,
 248 1999; Forrest et al., 2012), W_t is the weight at age t , ψ_t is the fraction of females that are mature
 249 at age t . Weight-at-age was estimated as function of the weight to length conversion parameters a
 250 and b and length-at-age, L_t , such that $W_t = aL_t^b$. The corresponding L_t for carpenter was
 251 calculated based on the Bertalanffy growth function parameters given in Brouwer and Griffiths
 252 (2006) (Table 1):

$$253 \quad L_t = L_\infty (1 - \exp(-k(t - t_0))),$$

254 while L_t for silver kob growth was calculated using the growth parameters of the Richards
 255 function (Schnute, 1981) provided by Griffiths (1997) (Table 1):

$$256 \quad L_t = L_\infty \left(1 + \frac{\exp(-k(t - t^*))}{p} \right)^{-p}.$$

257 The fraction of mature females at age t was calculated as a function of:

$$258 \quad \psi_t = \frac{1}{1 + \exp(-(t - t_{m50}) / \delta_t)},$$

259 where t_{m50} is the estimated age-at-50%-maturity (Table 1) and δ_t was set to 0.1 to resemble close

260 to knife-edge maturation. For the calculation of α first consider the Beverton and Holt spawner-

261 recruitment relationship (S-R) of the form:

$$262 \quad R = \frac{\alpha S}{1 + \beta S},$$

263 where R is the number of recruits, S is the spawner biomass and β is the scaling parameter

264 (Hilborn and Walters, 1992). In contrast to alternative formulations of the Beverton and Holt S-

265 R function, the parameter α can be directly interpreted as the slope in the origin of the S-R curve

266 (Hilborn and Walters, 1992). We re-parameterized α as function of unfished spawner-biomass

267 per recruit SPR_0 and the steepness parameter h of the spawner-recruitment relationship (Myers et

268 al., 1999; Forrest et al., 2012), such that:

$$269 \quad \alpha = \frac{4h}{(1-h)} SPR_0^{-1},$$

270 where h is defined as the ratio of recruitment at a spawner biomass that is reduced to 20% of

271 pristine levels to pristine recruitment (Mace and Doonan, 1988), and SPR_0 is a function of:

$$272 \quad SPR_0 = \left(\sum_{t=1}^{t_{max}-1} W_t \psi_t \exp(-M) \right) + W_{t_{max}} \psi_{t_{max}} \frac{\exp(-Mt_{max})}{1 - \exp(-M)},$$

273 where the maximum observed age, t_{max} , is treated as a plus group. In contrast to the population-

274 specific parameters α and β , the estimate of the steepness parameter h of the S-R relationship

275 has the advantage that it is directly comparable between populations (Hilborn and Liermann,

276 1998). This property permits to derive empirical Bayesian priors for h from meta-analyses of
277 multiple stocks (Myers et al., 1999; Dorn, 2002; Forrest et al., 2012). Myers et al. (1999), for
278 example, provided estimates of steepness h for 57 fish species, which they derived from a meta-
279 analysis of spawner-recruitment data for 249 populations. Because there was no specific
280 information on h for silver kob and carpenter available, we adapted a rather generic mean
281 steepness value of $h = 0.7$ for both species, which represents the overall average steepness value
282 derived for fairly long-lived, highly fecund fishes of medium to large body size (Myers et al.,
283 1999; Rose et al., 2001). Many commercially exploited species, including Sparidae and
284 Scianidae, typically fall into this ecological group of fishes (Winemiller, 1992; Myers et al.,
285 2002), which corresponds to the general domain of periodic life history strategists (Winemiller
286 and Rose, 1992).

287

288 Finally, a Monte-Carlo simulation procedure was used to generate prior distributions for r from
289 the Leslie-Matrix (McAllister et al., 2001). For this purpose, random variables of M and h were
290 drawn from a log-normal distribution, with $M = \mu_M \exp(\varepsilon - \sigma_{\ln}^2 / 2)$, $h = \mu_h \exp(\varepsilon - \sigma_{\ln}^2 / 2)$ and
291 $\varepsilon \sim N(0, \sigma_{\ln}^2)$. The variance parameters were set to achieve CV's of 20% for both M and h . For
292 each species, we generated a vector 1000 random r deviates. The parameters μ_r and σ_{\ln}^2 ,
293 defining the prior distribution for r , were derived by fitting a lognormal distribution to the
294 bootstrap vector. The resultant prior parameter estimates were $\mu_r = 0.18$ and $\sigma_{\ln}^2 = 0.27^2$ for
295 carpenter and $\mu_r = 0.21$ and $\sigma_{\ln}^2 = 0.26^2$ for silver kob (Table 1).

296

297

298 *Posterior distributions and uncertainty*

299 Joint posterior probability distributions of model parameters, projections and management

300 quantities were estimated using the Metropolis-Hastings Markov Chain Monte-Carlo (MCMC)

301 algorithm implemented for random effects models in ADMB-RE (Fournier et al., 2012).

302 Convergence of the MCMC chains was diagnosed using the coda package (Plummer et al., 2006)

303 implemented in the statistical software R (R Development Core Team, 2011), adopting minimal

304 thresholds of $p = 0.05$ for Geweke's diagnostic (Geweke, 1992) and the two-stage Heidelberger-

305 Welch stationary test (Heidelberger and Welch, 1992).

306

307 The mixing in the MCMC chains was generally fairly slow and often insufficient. The latter

308 appeared to be caused by non-stationary behaviour of the process error variance σ^2 . We therefore

309 introduced a double-logistic function as a penalty to constrain the ratio $V_R = \hat{\tau}^2 / \hat{\sigma}^2$ within the

310 boundaries by:

$$311 \quad p = \frac{1}{(1 + \exp(-(x - R_1) / \delta_{R1}))(1 + \exp(-(x - R_2) / \delta_{R2}))},$$

312 where $R_1 = \hat{V}_R / 2$, $R_2 = 2\hat{V}_R$, $\delta_{R1} = 0.02\hat{V}_R$, $\delta_{R2} = 0.04\hat{V}_R$ and \hat{V}_R denotes the ratio

313 unconstrained maximum likelihood estimates $\hat{V}_R = \hat{\tau}^2 / \hat{\sigma}^2$. The corresponding negative log-

314 likelihood profile, $-\ln(p)$, is illustrated for the example of $\hat{V}_R = 4$ (Fig. 2). This penalty increased

315 the stability of the MCMC chains substantially and convergence could be achieved for all base-

316 case models after running the MCMC simulation for 2 million cycles, discarding the first 200000

317 iterations as burn-in phase and then thinning the chain by saving every 200th iteration to reduce

318 autocorrelation.

319

320 The 2.5th and 97.5th percentiles of the posterior distributions are used to represent 95% Bayesian
321 credibility intervals for all parameters, projections and management quantities. The estimated
322 95% credibility intervals are analogous to 95% confidence intervals and can interpreted in the
323 sense that there is a 95% probability that the lower and upper credibility intervals includes the
324 true value given the prior information and the data.

325

326 **Results and discussion**

327 In 2000, a state of emergency was declared in the South African boat-based handline fishery on
328 the basis of substantially decreased catch rates of important species and alarming results from
329 spawner biomass per-recruit analyses. The emergency was accompanied by a significant
330 reduction in commercial line-boat effort to allow stock recovery. Declines in linefishery catches
331 of carpenter and silver kob were not uniform and generally commenced prior to the forced effort
332 reduction in 2000 and typically reached a minimum during the period 2001 - 2004 (Fig. 3).

333 Inshore trawl catches, by contrast, increased during this period, to the extent that they frequently
334 exceeded the linefishery catches during the first five years after the emergency (Fig. 3).

335

336 The model fits appeared to be adequate in that the models were able to predict the observed
337 increase in the standardized CPUE indices. The clearest and most consistent trends were evident
338 for southern-eastern stocks of carpenter (Fig. 4 A) and silver kob (Fig. 4 B), which was
339 supported by fairly narrow 95% credibility intervals. The fit to south coast silver kob data
340 showed moderate departures from the standardized CPUE indices in most recent years (Fig. 4 C).

341 The posterior medians for the intrinsic rate of population rate r were fairly similar for both
342 species but were found to be consistently lower than their corresponding priors means (Tables 1
343 and 3, Fig. 5). This could indicate a lower stock productivity than predicted by the species' life
344 history traits or perhaps points towards sources of additional fishing mortality that were not
345 accounted for by the available data. On intra-specific comparisons, the posterior medians for r
346 were slightly higher for the south-eastern coast stocks.

347

348 The models consistently predicted an improvement in biomass compared to levels around 2000,
349 as the drastic management intervention in the linefishery forced harvest rates below those at
350 Maximum Sustainable Yield (Figs. 6 and 7). The two silver kob stocks remain of concern as
351 inshore trawl catches have increased since 2000, slowing down potential recoveries and possibly
352 resulting in growth overfishing due to earlier selectivity.

353

354 **References**

355 Attwood, C.G., Petersen, S.L., Kerwath, S.E., 2011. Bycatch in South Africa's inshore trawl
356 fishery as determined from observer records. ICES Journal of Marine Science: Journal du
357 Conseil 68, 2163-2174.

358 Booth, A.J., Quinn II, T.J., 2006. Maximum likelihood and Bayesian approaches to stock
359 assessment when data are questionable. Fisheries Research (Amsterdam) 80, 169-181.

360 Brodziak, J., Ishimura, G., 2012. Development of Bayesian production models for assessing the
361 North Pacific swordfish population. Fish. Sci. 77, 23-34.

- 362 Brouwer, S.L., Griffiths, M.H., 2006. Management of *Argyrozona argyrozona* (Pisces: Sparidae)
363 in South Africa based on per-recruit models. *Afr. J. Mar. Sci.* 28, 89-98.
- 364 Buckland, S.T., Newman, K.B., Thomas, L., Koesters, N.B., 2004. State-space models for the
365 dynamics of wild animal populations. *Ecol. Model.* 171, 157-175.
- 366 Butterworth, D.S., De Oliveira, J.A.A., Cochrane, K.L., 1993. Current initiatives in refining the
367 management procedure for the South African anchovy resource. University of Alaska Fairbanks.
368 Proceedings of the International Symposium on Management Strategies for Exploited Fish
369 Populations., Alaska Sea Grant College Program Report No. 93-02, Fairbanks, Alaska, pp. 439–
370 473.
- 371 Butterworth, D.S., Punt, A.E., Borchers, D.L., Pugh, J.B., Hughes, G.S., 1989. A manual of
372 mathematical techniques for linefish assessment. SANCOR. South African National Scientific
373 Programmes Report 160, Cape Town, p. 89.
- 374 Buxton, C.D., 1992. The application of yield-per-recruit models to two South African sparid reef
375 species, with special consideration to sex change. *Fish. Res.* 15, 1-16.
- 376 Caswell, H., 2001. Matrix population models: Construction, analysis and interpretation. Sinauer
377 Associates, Sunderland, Massachusetts.
- 378 Chaloupka, M., Balazs, G., 2007. Using Bayesian state-space modelling to assess the recovery
379 and harvest potential of the Hawaiian green sea turtle stock. *Ecol. Model.* 205, 93-109.
- 380 de Valpine, P., 2002. Review of Methods for Fitting Time-Series Models with Process and
381 Observation Error and Likelihood Calculations for Nonlinear, Non-gaussian State-Space Models.
382 *Bull. Mar. Sci.* 70, 455-471.
- 383 Dorn, M.W., 2002. Advice on West Coast rockfish harvest rates from Bayesian meta-analysis of
384 stock-recruit relationships. *N. Am. J. Fish. Manage.* 22, 280-300.

- 385 Forrest, R.E., McAllister, M.K., Dorn, M.W., Martell, S.J.D., Stanley, R.D., 2012. Hierarchical
386 Bayesian estimation of recruitment parameters and reference points for Pacific rockfishes
387 (*Sebastes* spp.) under alternative assumptions about the stock-recruit function. Canadian Journal
388 of Fisheries & Aquatic Sciences 67, 1611-1634.
- 389 Fournier, D.A., Skaug, H.J., Ancheta, J., Ianelli, J., Magnusson, A., Maunder, M.N., Nielsen, A.,
390 Sibert, J.R., 2012. AD Model Builder: using automatic differentiation for statistical inference of
391 highly parameterized complex nonlinear models. Optimization Methods and Software 27, 233-
392 249.
- 393 Geweke, J., 1992. Evaluating the accuracy of sampling-based approaches to the calculation of
394 posterior moments. In: Berger, J.O., Bernardo, J.M., Dawid, A.P., Smith, A.F.M.s (Eds.),
395 Bayesian Statistics 4: Proceedings of the Fourth Valencia International Meeting. Clarendon
396 Press, Oxford, pp. 169–193.
- 397 Griffiths, M.H., 1997. The application of per-recruit models to *Argyrosomus inodorus*, an
398 important South African sciaenid fish. Fish. Res. 30, 103-115.
- 399 Griffiths, M.H., 2000. Long-term trends in catch and effort of commercial linefish off South
400 Africa's Cape Province: snapshots of the 20th century South African Journal of Marine Science
401 22, 81-110.
- 402 Heidelberger, P., Welch, P., 1992. Simulation run length control in the presence of an initial
403 transient. Operations Research 31, 1109–1144.
- 404 Hilborn, R., Liermann, M., 1998. Standing on the shoulders of giants: learning from experience
405 in fisheries. Rev. Fish Biol. Fish. 8, 273-283.
- 406 Hilborn, R., Walters, C.J., 1992. Quantitative fisheries stock assessment: choice, dynamics and
407 uncertainty. Chapman and Hall, New York.

- 408 Mace, P.M., Doonan, I.J., 1988. A generalized bioeconomic simulation model for fish population
409 dynamics. New Zealand Fishery Assessment, Research Document, 88/4, p. 51
- 410 McAllister, M.K., Kirkwood, G.P., 1998. Bayesian stock assessment: a review and example
411 application using the logistic model. *ICES J. Mar. Sci.* 55, 1031-1060.
- 412 McAllister, M.K., Pikitch, E.K., Babcock, E.A., 2001. Using demographic methods to construct
413 Bayesian priors for the intrinsic rate of increase in the Schaefer model and implications for stock
414 rebuilding. *Can. J. Fish. Aquat. Sci.* 58, 1871-1890.
- 415 Meyer, R., Millar, C.P., 1999. BUGS in Bayesian stock assessments. *Can. J. Fish. Aquat. Sci.* 56,
416 1078–1086.
- 417 Millar, C.P., Meyer, R., 2000. Non-linear state space modelling of fisheries biomass dynamics
418 Metropolis-Hastings within-Gibbs sampling. *Applied Statistics* 49, 327-342.
- 419 Mollet, H.F., Cailliet, G.M., 2002. Comparative population demography of elasmobranchs using
420 life history tables, Leslie matrices and stage-based matrix models. *Marine and Freshwater
421 Research* 53, 503-515.
- 422 Myers, R.A., Barrowman, N.J., Hilborn, R., Kehler, D.G., 2002. Inferring Bayesian Priors with
423 Limited Direct Data: Applications to Risk Analysis. *N. Am. J. Fish. Manage.* 22, 351-364.
- 424 Myers, R.A., Bowen, K.G., Barrowman, N.J., 1999. Maximum reproductive rate of fish at low
425 population sizes. *Can. J. Fish. Aquat. Sci.* 56, 2404-2419.
- 426 Ono, K., Punt, A.E., Rivot, E., 2012. Model performance analysis for Bayesian biomass
427 dynamics models using bias, precision and reliability metrics. *Fish. Res.* 125, 173-183.
- 428 Pedersen, M.W., Berg, C.W., Thygesen, U.H., Nielsen, A., Madsen, H., 2012. Estimation
429 methods for nonlinear state-space models in ecology. *Ecol. Model.* 222, 1394-1400.

- 430 Plummer, M., Nicky Best, Cowles, K., Vines, K., 2006. CODA: Convergence Diagnosis and
431 Output Analysis for MCMC. R News 6, 7-11
- 432 Polachek, T., Hilborn, R., Punt, A.E., 1993. Fitting surplus production models: comparing
433 methods and measuring uncertainty. Can. J. Fish. Aquat. Sci. 50, 2598-2607.
- 434 Punt, A.E., 1993. The use of spawner-biomass-per-recruit in the management of linefisheries.
435 Special Publication of the Oceanographic Research Institute, Durban 2, 80-89.
- 436 Punt, A.E., 2003. Extending production models to include process error in the population
437 dynamics. Can. J. Fish. Aquat. Sci. 60, 1217-1228.
- 438 Punt, A.E., Hilborn, R.A.Y., 1997. Fisheries stock assessment and decision analysis: the
439 Bayesian approach. Rev. Fish Biol. Fish. 7, 35-63.
- 440 Punt, A.E., Pulfrich, A., Butterworth, D.S., Penney, A.J., 1996. The effect of hook size on the
441 size-specific selectivity of hottentot *Pachymetopon blochii* (Val.) and on yield per recruit South
442 African Journal of Marine Science 17, 155-172.
- 443 Quinn, T.J., Deriso, R.B., 1999. Quantitative fish dynamics. Oxford University Press, New York.
- 444 R Development Core Team, 2011. R: A language and environment for statistical computing. R
445 Foundation for Statistical Computing, Vienna.
- 446 Rose, K.A., Cowan Jr, J.H., Winemiller, K.O., Myers, R.A., Hilborn, R., 2001. Compensatory
447 density dependence in fish populations: importance, controversy, understanding and prognosis.
448 Fish Fish. 2, 293-327.
- 449 Schnute, J., 1981. A versatile growth model with statistically stable parameters. Can. J. Fish.
450 Aquat. Sci. 38, 1128-1140.

451 Thorson, J.T., Cope, J.M., Branch, T.A., Jensen, O.P., 2012. Spawning biomass reference points
452 for exploited marine fishes, incorporating taxonomic and body size information. *Can. J. Fish.*
453 *Aquat. Sci.* 69, 1556-1568.

454 Winemiller, K.O., 1992. Life history and the effectiveness of sexual selection. *Oikos* 63, 318-
455 327.

456 Winemiller, K.O., Rose, K.A., 1992. Patterns of life-history diversification in North American
457 fishes: implications for population regulation. *Can. J. Fish. Aquat. Sci.* 49, 2196-2218.

458 Winker, H., Kerwath, S.E., Attwood, C.G., 2012. Report on stock assessments of important
459 South African linefish resources. Report of the Linefish Scientific Working Group, LSWG No.
460 3, 2012. Department of Agriculture, Forestry and Fisheries, Cape Town, p. 65.

461 Winker, H., Kerwath, S.E., Attwood, C.G., accepted. Comparison of two approaches to
462 standardize catch-per-unit-effort for targeting behaviour in a
463 multispecies hand-line fishery. *Fish. Res.*

464 Zhou, S., Punt, A.E., Deng, R., Dichmont, C.M., Ye, Y., Bishop, J., 2009. Modified hierarchical
465 Bayesian biomass dynamics models for assessment of short-lived invertebrates: a comparison for
466 tropical tiger prawns. *Marine and Freshwater Research* 60, 1298–1308.

467

468

469

470

471

472

473

474 **Table 1** Summary of prior probability density functions used to fit Bayesian state-space models
 475 to data from carpenter and silver kob stocks

Prior type	Carpenter	Silver Kob
Non-informative	$K \sim \text{inversegamma}(0.001, 0.001)$	$K \sim \text{inversegamma}(0.001, 0.001)$
Informative	$r \sim \text{Lognormal}(-1.746, 0.266)$	$r \sim \text{Lognormal}(-1.551, 0.258)$
Informative	$\varphi \sim \text{Lognormal}(-1.897, 0.385)$	$\varphi \sim \text{Lognormal}(-2.659, 0.385)$
Non-informative	$\ln(q) \sim \text{Uniform}(-10, 2)$	$\ln(q) \sim \text{Uniform}(-10, 2)$
Non-informative	$\sigma^2 \sim \text{inversegamma}(0.001, 0.001)$	$\sigma^2 \sim \text{inversegamma}(0.001, 0.001)$
Non-informative	$\tau^2 \sim \text{inversegamma}(0.001, 0.001)$	$\tau^2 \sim \text{inversegamma}(0.001, 0.001)$

476

477

478 **Table 2** Summary of life history parameters used to derive informative priors for the intrinsic
 479 rate of population increase r .

Species	Parameter	Value	Source
Carpenter	L_{∞}	619 mm FL	Brouwer & Griffith (2005)
	k	0.06 year ⁻¹	Brouwer & Griffith (2005)
	t_0	-4.5 years	Brouwer & Griffith (2005)
	a	0.00004 g	Brouwer & Griffith (2005)
	b	2.924 g mm ⁻¹	Brouwer & Griffith (2005)
	M	0.10 year ⁻¹	Brouwer & Griffith (2005)
	t_{m50}	4 years	Brouwer & Griffith (2005)
	δ_t	0.10 year ⁻¹	assumed ~ knife-edge
	t_{\max}	30 years	Brouwer & Griffith (2005)
Silver Kob	L_{∞}	1142 mm FL	Griffiths (1997)
	k	0.65 year ⁻¹	Griffiths (1997)
	t^*	-4.5 years	Griffiths (1997)
	ρ	0.26	Griffiths (1997)
	a	0.000006 g	Griffiths (1997)
	b	3.07 g mm ⁻¹	Griffiths (1997)
	M	0.15 year ⁻¹	Griffiths (1997)
	t_{m50}	2.4 years	Griffiths (1997)
	δ_t	0.10 year ⁻¹	assumed ~ knife-edge
	t_{\max}	30 years	Griffiths (1997)

480

481

482

483

484

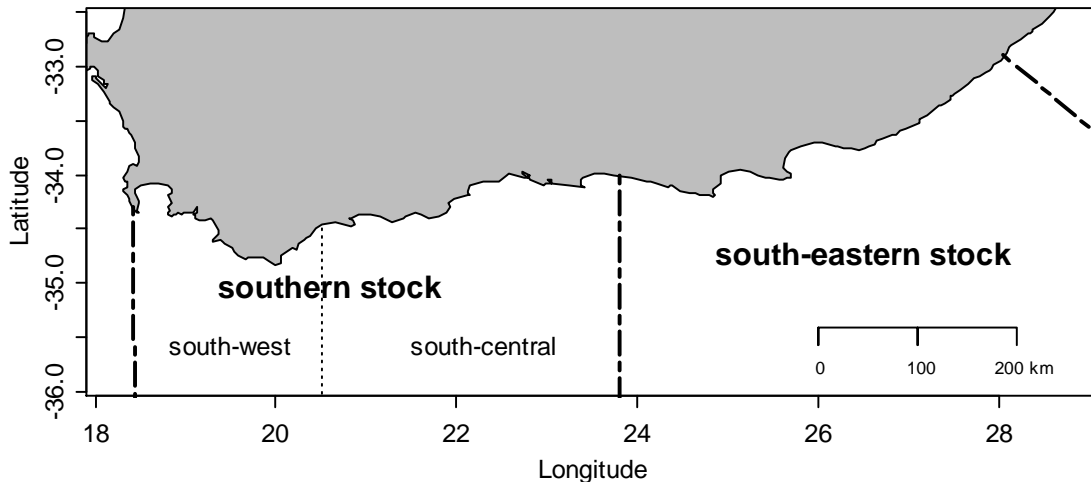
485

486 **Table 3.** Posterior means and 95% Bayesian credibility intervals for the southern and south-
 487 eastern carpenter and silver kob stocks.

Parameters	Carpenter southern stock		Silver kob southern stock	
	Median	95% Credibility Interval	Median	95% Credibility Interval
K	23335.0	10722.1 - 52505.5	107285.0	45752.2 - 239456.0
r	0.149	0.117 - 0.210	0.097	0.072 - 0.128
ϕ	0.182	0.085 - 0.351	0.087	0.042 - 0.200
q_{SW}	0.015	0.012 - 0.018	0.006	0.004 - 0.009
q_{SC}	0.020	0.016 - 0.025	0.010	0.007 - 0.014
σ^2	0.00097	0.00039 - 0.00254	0.0010	0.0005 - 0.0021
τ_{SW}^2	0.00556	0.00197 - 0.01353	0.0120	0.0059 - 0.0241
τ_{SC}^2	0.00562	0.00204 - 0.01396	0.0146	0.0086 - 0.0272
MSY	863.2	554.4 - 1644.0	2571.0	1285.1 - 5130.3
H_{MSY}	0.075	0.059 - 0.105	0.048	0.036 - 0.064
B_{MSY}	11667.5	5361.0 - 26252.7	53642.5	22876.1 - 119728.0
B_{2012}/K	0.361	0.173 - 0.644	0.1269	0.0605 - 0.2895
B_{2012}/B_{2000}	2.328	2.02 - 2.69	1.56	1.41 - 1.76
Parameters	Carpenter south-eastern stock		Silver kob southern-eastern stock	
	Median	95% Credibility Interval	Median	95% Credibility Interval
K	23588.8	11922.5 - 50836.0	30543.5	14802.9 - 66970.5
r	0.164	0.121 - 0.211	0.141	0.109 - 0.178
ϕ	0.120	0.12 - 0.059	0.075	0.075 - 0.036
q_{SE}	0.023	0.013 - 0.031	0.024	0.016 - 0.032
σ^2	0.00208	0.00090 - 0.00481	0.00092	0.00039 - 0.0023
τ_{SE}^2	0.01109	0.00592 - 0.02221	0.00522	0.00244 - 0.0112
MSY	959.8	567.7 - 567.7	1067.1	577.5 - 2123.1
H_{MSY}	0.082	0.060 - 0.105	0.070	0.055 - 0.089
B_{MSY}	11794.4	5961.25 - 25418.0	15271.8	7401.5 - 33485.2
B_{2012}/K	0.394	0.207 - 0.667	0.178	0.085 - 0.349
B_{2012}/B_{2000}	3.440	2.80 - 4.23	2.44	2.10 - 2.86

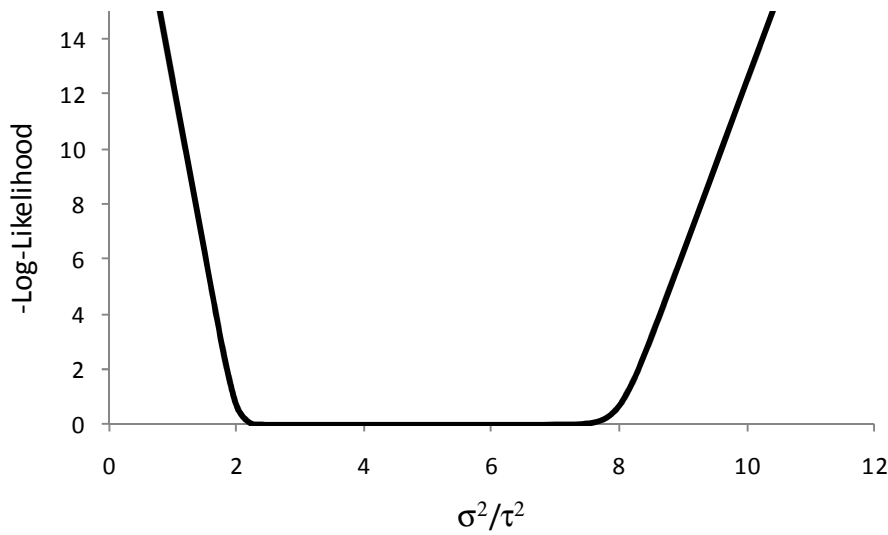
488

489

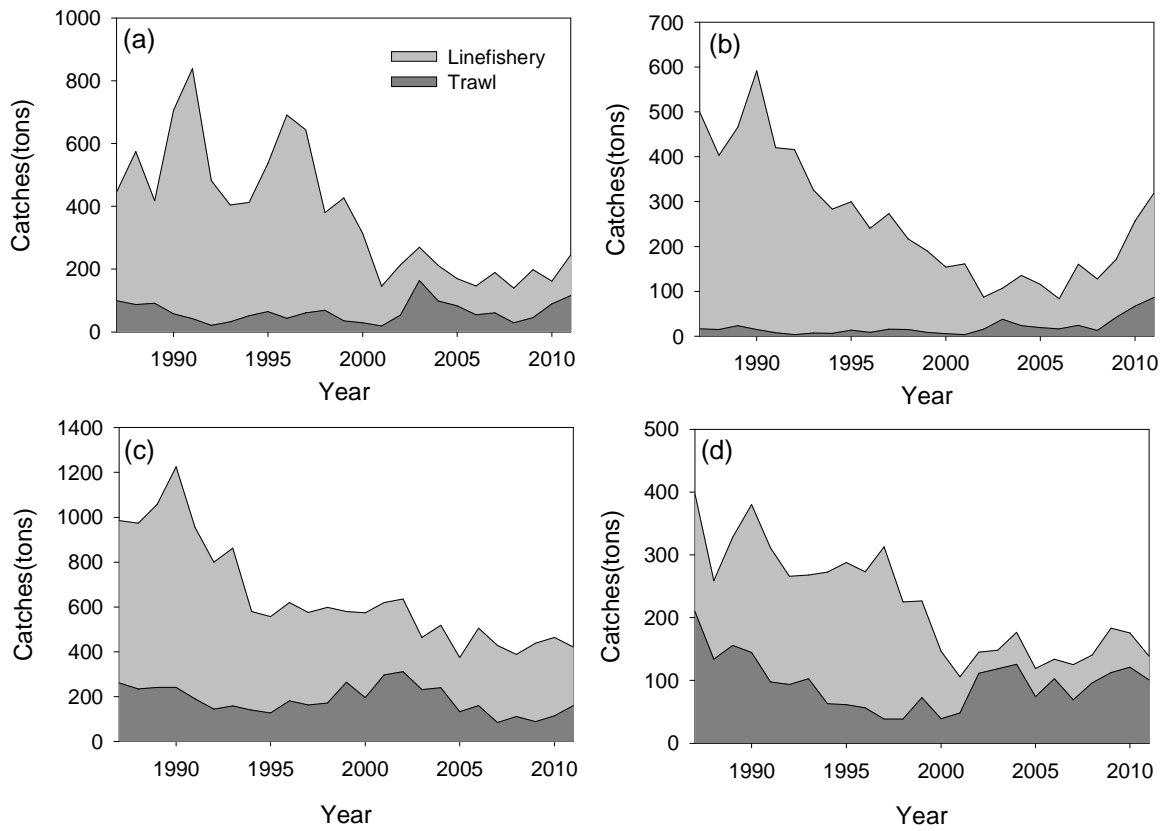


490 **Fig.1** Map showing the regional split for southern and south-eastern stocks of carpenter and
 491 silver kob.
 492

493
 494



495 **Fig. 2** illustrating a negative log-likelihood profile for used as penalty to stabilize the MCMC
 496 runs. The example is based on $\hat{V}_R = \hat{\tau}^2 / \hat{\sigma}^2 = 4$ (see text).
 497

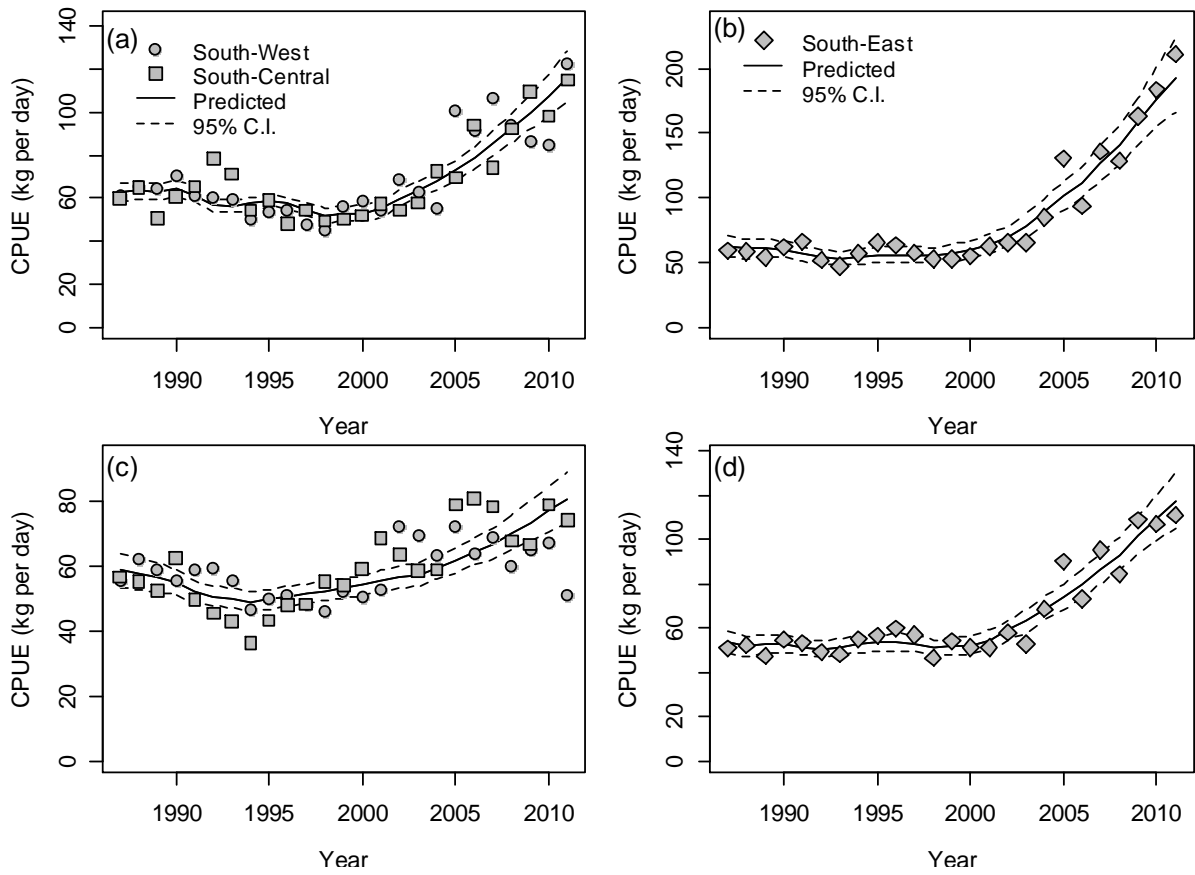


498

499 **Fig. 3** Cumulative area plots illustrating total catches (tons) by sector for (a) carpenter south, (b)

500 carpenter east, (c) silver kob south and (d) silver kob east

501



502

503 **Fig. 4** Standardized CPUE indices and model fits for (a) carpenter south, (b) carpenter south-

504 east, (c) silver kob south and (d) silver kob south-east. Note that the CPUE from the south-

505 central CPUE was scaled to the CPUE from the south-west coast by applying the estimated

506 catchability coefficients.

507

508

509

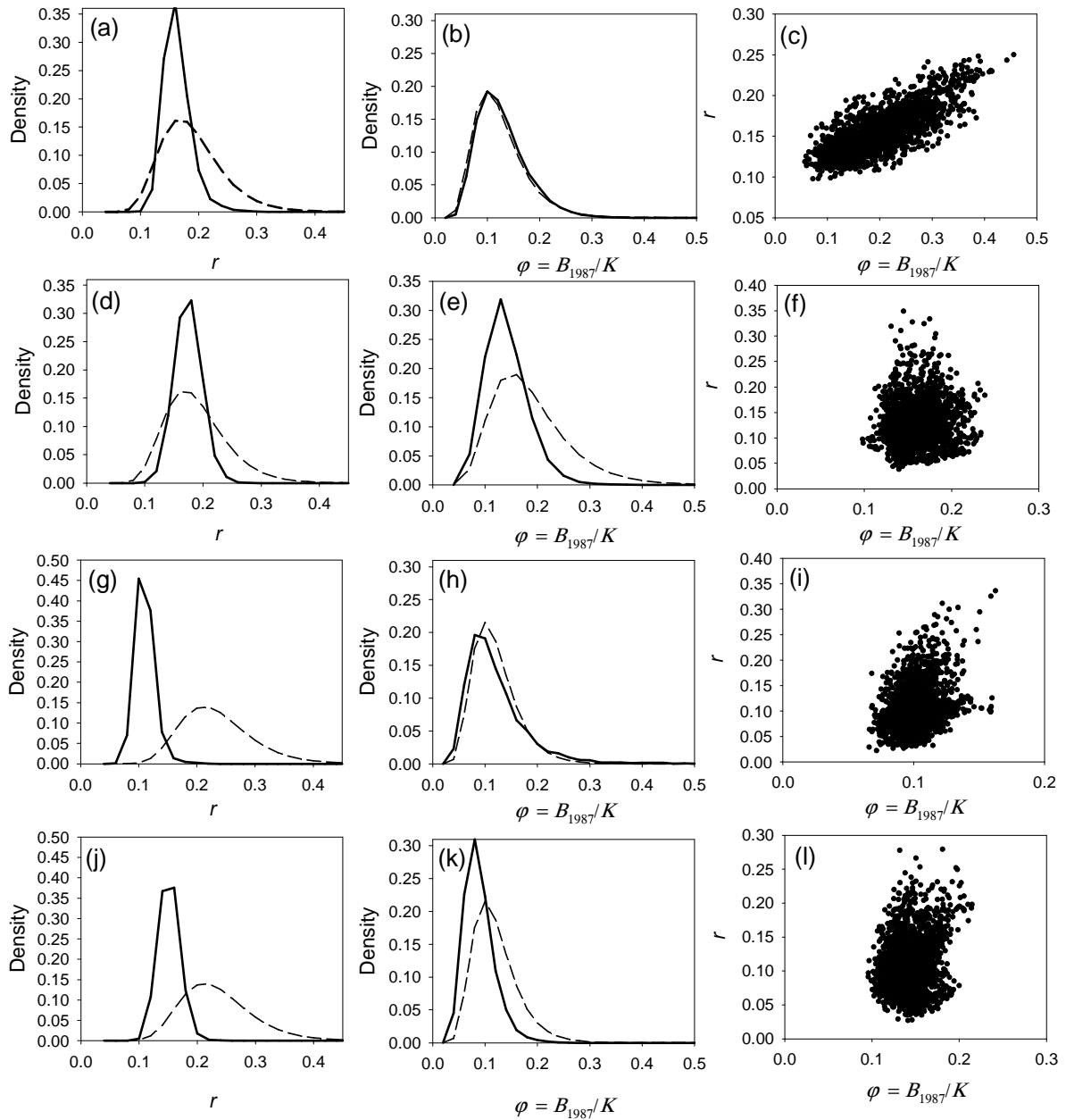
510

511

512

513

514



515

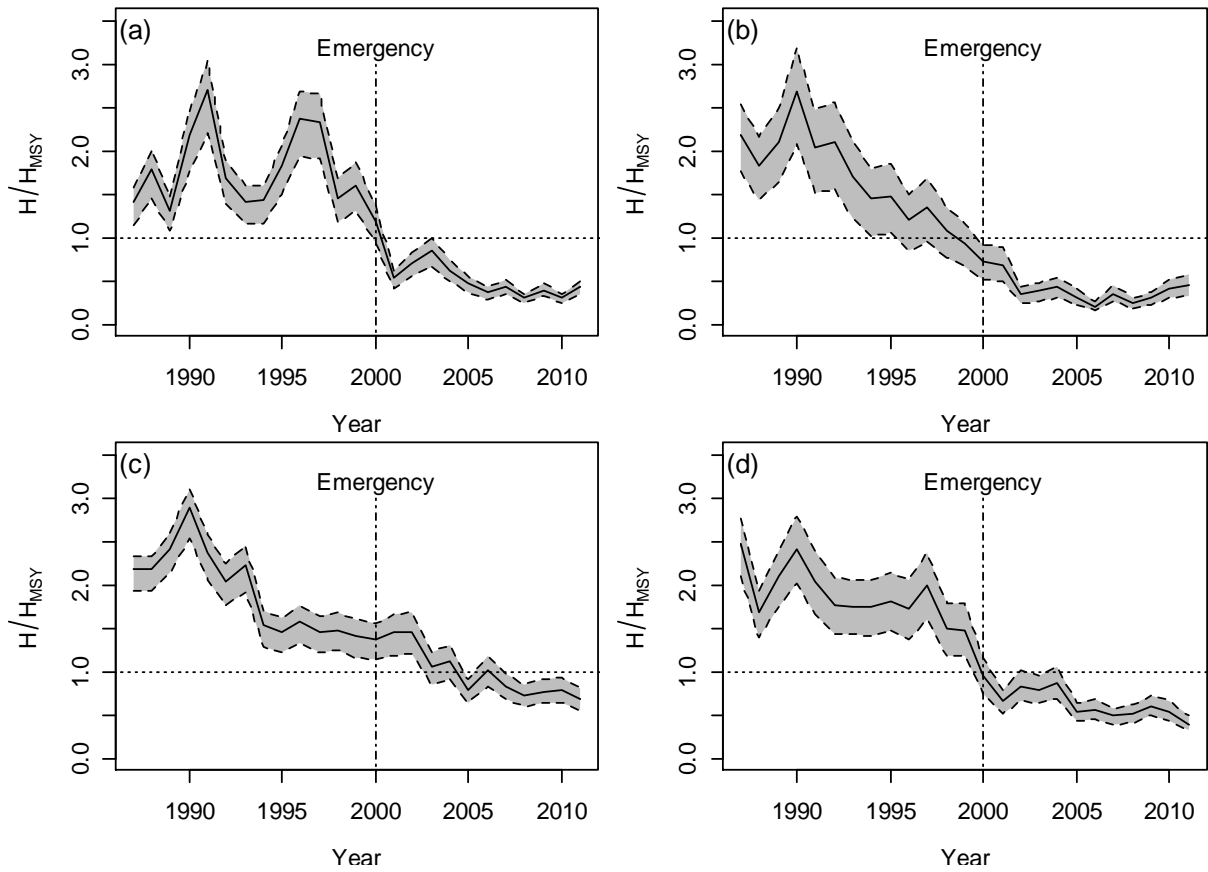
516 **Fig. 5** Informative prior and joint posterior distributions for carpenter south (a) – (c), carpenter

517 south-east (d) – (f), silver kob south (g) – (i) and silver kob south-east (j) – (l).

518

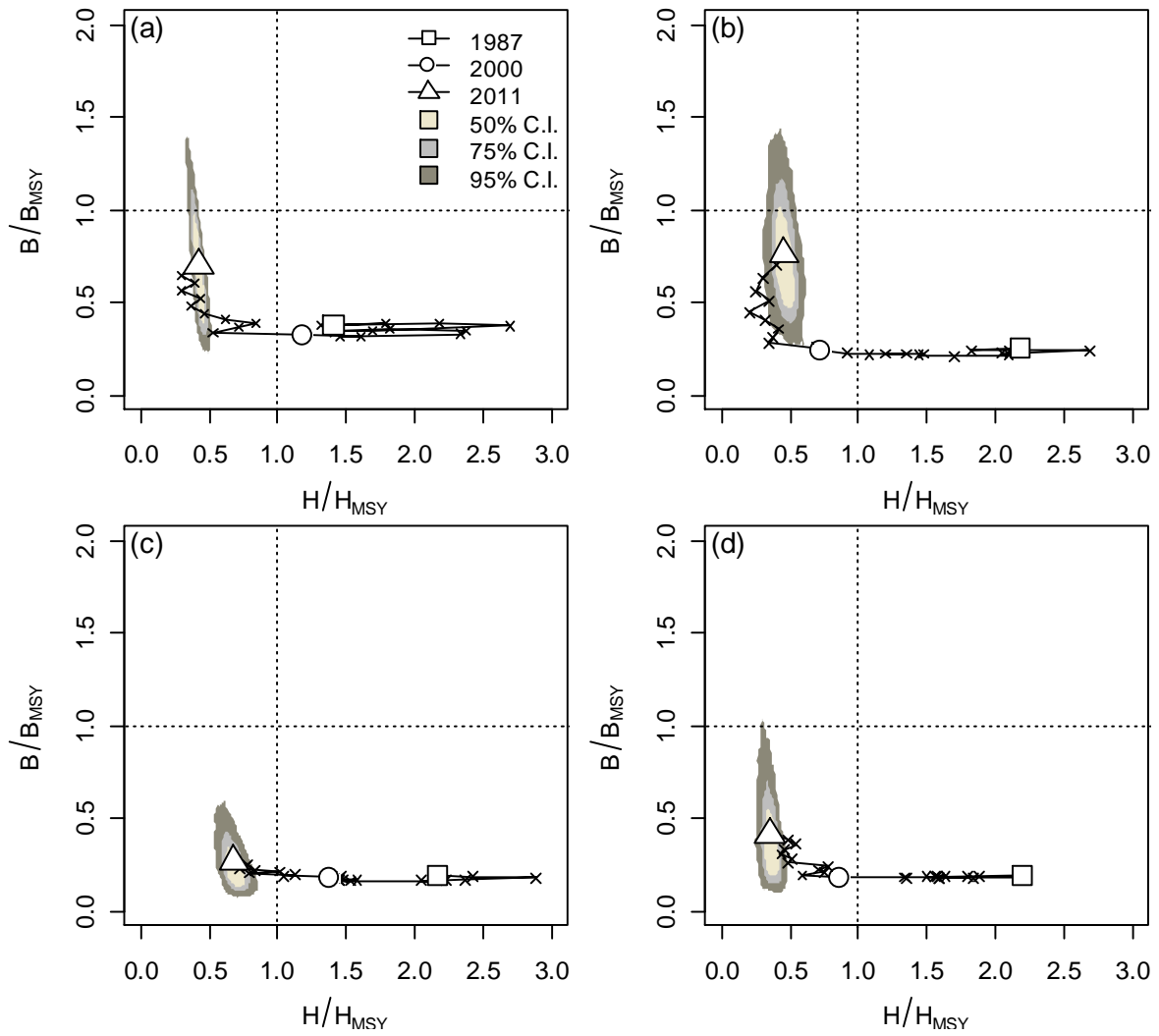
519

520



521

522 **Fig. 6** Ratio harvest rate to HMSY for (a) carpenter south, (b) carpenter south-east, (c) silver kob
 523 south and (d) silver kob south-east. The gray shaded areas illustrate the 95% credibility
 524 intervals.



525

526 **Fig. 7** Biplots illustrating the predicted trajectories of the ratios B/B_{MSY} and H/H_{MSY} for (a)
 527 carpenter south, (b) carpenter east, (c) silver kob south and (d) silver kob east. The shaded areas
 528 show kernel densities representing the 50%, 75% and 95% credibility intervals.

529

530

531